

Cloud-Native Vector Search: A Comprehensive Performance Analysis [Experiments, Analysis and Benchmark]

Zhaoheng Li*, Wei Ding[†], Silu Huang[†], Zikang Wang[†], Yuanjin Lin[†], Ke Wu[†], Yongjoo Park*, Jianjun Chen[†]

University of Illinois Urbana-Champaign* Bytedance[†]

{zlh20,yongjoo}@illinois.edu,{wei.ding,silu.huang,wangzikang,linyuanjin,ke.wu,jianjun.chen}@bytedance.com

ABSTRACT

Vector search has been widely employed in recommender system and retrieval-augmented-generation pipelines, commonly performed with *vector indexes* to efficiently find similar items in large datasets. Recent growths in both data and task complexity have motivated placing vector indexes onto remote storage—*cloud-native vector search*, which cloud providers have recently introduced services for. Yet, despite varying workload characteristics and various available vector index forms, providers default to using *cluster-based* indexes, which on paper do not adapt well to differences between disk and cloud-based environment: their fetch granularities and lack of notable intra-query dependencies align with the large optimal fetch sizes and minimizes costly round-trips (i.e., as opposed to *graph-based* indexes) to remote storage, respectively.

This paper systematically studies cloud-native vector search: *What and how should indexes be built and used for on-cloud vector search?* We analyze bottlenecks of two common index classes, cluster and graph indexes, on remote storage, and show that despite current standardized adoption of cluster indexes on the cloud, graph indexes are favored in workloads requiring high concurrency and recall, or operating on high-dimensional data or large datatypes. We further find that on-cloud search demands significantly different indexing and search parameterizations versus on-disk search for optimal performance. Finally, we incorporate existing cloud-based caching setups into vector search and find that certain index optimizations *work against* caching, and study how this can be mitigated to maximize gains under various available cache sizes.

1 INTRODUCTION

Finding semantically similar items via *vector search* is a cornerstone of many recent recommender systems and retrieval-augmented-generation (RAG) pipelines [46, 49, 70, 82]. The problem of doing so efficiently, with *vector indexes*, has gained popularity as usage of large-scale vector datasets [9, 33] become feasible via efficient embedding models [51, 56, 67]. Oftentimes, depending on task specifications, the index may reside in different locations: it may need to be *in-memory* for applications demanding sub-millisecond latency (e.g., fraud detection [68]), while tasks focused on cost-effectiveness (e.g., eCommerce [45]) may prefer indexes to be *on-disk*.

Emergence of Cloud-Native Vector Search. Recently, as data scales demanded by vector search grow even larger (e.g., Bing Visual Search [11] and eBay Recommendations’ [23] billion-scale datasets), providers such as TurboPuffer [77] and Amazon S3 Vector [12] have begun offering cloud-native vector search services, providing cost-efficient solutions for storing and querying these

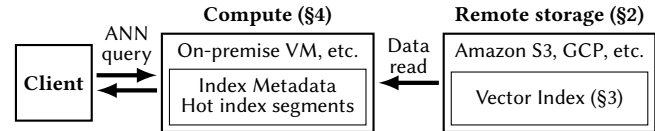


Figure 1: Cloud-native vector search setup we study in this paper. Compute fetches vector index segments from remote storage and utilizes local resources to cache hot segments.

massive vector datasets by storing them and their indexes on remote storage. Fig 1 depicts a typical pipeline: vector indexes are stored as (immutable) *objects* on remote storage, then, clients interact with *compute* which performs ANN queries by fetching index *segments* for computation, while using local resources (e.g., memory, SSD) for caching (e.g., storing metadata of hot indexes [66]).

Current Providers Default to Cluster Indexes. There currently exists two distinct commonly-used index classes for vector search: *cluster indexes* based on inverted lists for text search [93] which organize datasets into KMeans-clustered posting lists, and *graph indexes*, which build KNN-like graphs over datasets and serve queries via iterative graph traversal. Despite the wide variety of workloads with different characteristics and requirements (e.g., dataset size, recall, latency, and throughput), almost all current on-cloud vector search providers offer only cluster indexes (e.g., IVF-PQ [60], SPANN [17], SPFresh [85]). In principle, cluster indexes’ search characteristics align with recent findings on remote storage performance [22, 27, 34]: Data is read at posting list (often tens of KBs in size) granularity from cluster indexes which matches the large (8-16MiB) cost/throughput-optimal fetch sizes, and the typical lack of intra-query dependencies—all required posting lists can be fetched at once—minimizes long roundtrip times (millisecond level) to remote storage. Yet, prior studies for on-disk indexing, which is highly similar with on-cloud search interface-wise (i.e., compute fetches required index *blocks* from disk), have shown that some workloads significantly favor graph indexes, with notable examples being high recall and/or throughput scenarios [18, 69].

Our Goal: How to Optimize Cloud-Native Vector Search? Hence, we hypothesize that unlike the one-size-fits-all cluster index-based approach of current providers, different workloads and setups call for different indexing choices, which we study in this paper: *What and how should vector indexes be built and used for cloud-native vector search?* We analyze bottlenecks faced by cluster and graph indexes for on-cloud search to answer the following sub-questions:

(RQ1) What index for what scenario? We aim to identify the optimal index class given dataset characteristics and query throughput, recall, latency, concurrency requirements. We show

that graph indexes could be favored in high concurrency and/or recall scenarios (e.g., Agentic AI tasks [76]) and vice versa (e.g., ad-hoc recommendations [11]). More interestingly, low dataset dimensions (e.g., 96D GIST descriptors [4]) and datatypes (e.g., INT8 [58]) shift the balance in favor of graph indexes.

(RQ2) How to design indexes? Cluster and graph indexes can be built in ways that vary in characteristics such as the amount of computation and data read per query. We aim to identify the optimal parameterization based the remote storage’s characteristics (e.g., I/O bandwidth). We find that, for cloud-native vector search, parameterization should prioritize reducing I/O, even if this substantially increases compute costs (such as by using more fine-grained posting lists for graph indexes). Notably, such configurations are often documented as suboptimal for on-disk indexing [17, 21].

(RQ3) How to utilize caching? Caching for vector search is relatively understudied, with existing providers [77] and works [91] defaulting to maximizing cache hit rate as proxy for performance. We study *how* indexes benefit from caching, and interestingly find that some indexing optimizations diminish caching gains (e.g., DiskANN’s multi-neighbor expansion), where higher cache hit rate does not directly lead to lower latency: Optimal indexing parameterizations (e.g., SPANN’s replication factor [17]) can heavily depend on cache size, and certain sizes may call for these optimizations to be *tuned down* to maximize caching gains for on-cloud search.

Contributions. According to our observations on the characteristics of existing and hypothetical cloud-native vector search pipelines (§2), we contribute the following with our benchmark study:

- (1) **Index Design (§3):** We follow our theory-driven modeling and bottleneck analysis of graph and cluster vector indexes for cloud-native vector search to formulate hypotheses on optimal indexing designs and parameterizations.
- (2) **Index-Cache Integration (§4):** We explore integrating caching methods of prior on-disk indexing and adjacent cloud analytics works into cloud-native vector search, identify missed opportunities, and hypothesize on how to improve caching gains.
- (3) **Experimental Evaluation (§5):** We perform extensive evaluation on 4 real-world vector datasets on realistic on-cloud and on-disk setups. We provide actionable insight on *what index to use* and *how to use them* in a wide variety of scenarios differing in recall/throughput/latency requirements, query concurrency, dataset characteristics, network resources, and cache size.

2 CLOUD VECTOR SEARCH FUNDAMENTALS

Recent *cloud-native* vector search architectures feature significant differences versus prior vector search works utilizing cloud storage [5, 31]. We will describe the key characteristics of this emerging framework in §2.1, then, its architectural bottlenecks in §2.2, then, the bottlenecks’ implications for on-cloud vector search in §2.3.

2.1 Cloud-Native Architecture

Cloud-based vector search setups have been explored by a variety of providers such as Manu [31], Milvus [79], and OpenSearch [5]. These works follow the commonly used practice in prior shared-architecture DBMSes [52, 86] and visualization dashboards [24, 88] of completely separating compute and storage: indexes are built and held on dedicated compute nodes for querying [31], and are

Table 1: Key differences of the specific remote storage and SSD we use for experimentation (§5) in this paper.

Storage	p50 Read Latency	GET QPS	Read Throughput (GB/s)
SSD	66.5 μ s	420,000	12
Volcano TOS [14]	9000 μ s	20,000	0.625

streamed to remote storage for persistence. While this approach offers high ad-hoc query performance as indexes are queried in-memory, costs can be high when large-scale datasets are involved.

Object Storage-First: Significant Cost Savings. Accordingly, TurboPuffer [77] and Amazon S3 Vector [12] have proposed the object storage-first, cloud-native vector search architecture that focuses on cost savings for large-scale workloads. These frameworks treat remote storage (e.g., Amazon S3 [2], Azure Blob [53], GCP [29], and Volcano TOS [14]) as the truth source on which indexes are stored. Then, instead of querying indexes in-memory, they follow similar procedures as querying on-disk indexes (e.g., DiskANN [21]), where required index *segments* (i.e., analogous to disk-based *blocks*, e.g., posting lists for the SPFresh index [85] utilized by TurboPuffer [77]) are fetched for querying. Then, local resources on compute nodes (e.g., memory, SSD) can be used as a cache for hot index segments, for example, TurboPuffer currently caches the cluster metadata (namely the BKT tree, §2.3.1) of commonly accessed SPFresh indexes. While this approach in general results in higher query latency due to incurring roundtrips to remote storage for fetching data that may be cold, operation costs are reduced (10-100 \times [77]) as indexes no longer need to be in-memory: storing indexes in remote storage is significantly cheaper (\sim 20\$ / TB / month [1, 14]).

2.2 Cloud Environments: Constrained I/O

Despite remarkably similar procedures between querying indexes on disk and remote storage—existing disk-based indexes such as DiskANN and SPANN can be queried *as is* when uploaded to remote storage (e.g., via mounting APIs [57]), the environment differences significantly affect performance of cloud-native vector search (Fig 3). This section describes I/O characteristics of remote storage that constrain cloud-native vector search performance. We present characteristics of the remote storage (Volcano TOS [14]) and local SSD we use for experiments (§5) in this paper for reference in Table 1.

Low Read Throughput. Read throughput from remote storage to the compute node is determined primarily by two factors: ingress bandwidth of compute controlled by its network interface card, and the throughput limit of the remote storage prefix holding the vector index.¹ Providers often limit the latter by throttling I/O due to shared infrastructure [2], with the specific limit often depending on compute location—on-premise machines use *internal network*, which typically has higher throughput (e.g., up to 50Gbps [7, 15]), while machines that access through *external network* are subject to lower throughputs (e.g., up to 5Gbps [15, 34]). In general, remote storage throughput is significantly lower versus local SSDs (up to 15GB/s [32]); hence, disk-based indexes may exhibit throughput bottlenecks on remote storage (§2.3.1).

¹All existing cloud-native vector search providers use one-compute-node-to-one-storage-bucket setups. We defer studying distributed setups to future work.

(a) **Most significant overhead categories of SPANN indexing configurations on-disk on the GIST1M dataset with $nprobe=8$ and concurrency=1.**

Index Location	I/O%	Distance Comps %	BKT Tree%
Disk	31.23	51.23	7.88
Remote Storage	54.16	28.99	6.10

(b) **Most significant overhead categories of DiskANN indexing configurations on-disk on the GIST1M dataset with $search_len=10$ and concurrency=1.**

Index Location	I/O%	Memory Operations %	PQ Distance Comps.%
Disk	68.69	11.20	7.80
Remote Storage	70.74	11.27	11.13

Figure 2: Key overheads of SPANN and DiskANN on GIST1M measured with perf [20]. Both indexes’ search costs are dominated by I/O, albeit different aspects of it, on remote storage.

Long Read Latency. The read latency of fetching data from remote storage to the compute node is determined by the hotness of the data segment being fetched: cold data (e.g., ad-hoc queries) incurs latency of 30-200ms, while hot, frequently-accessed data (e.g., long-tailed accesses of TurboPuffer’s Agentic AI workloads [76]) incurs latency as low as 10ms [22, 74]. Even for hot data, these numbers are still significantly larger than the 10-100 μ s of recent SSDs [43, 81], which degrades the performance of disk-based indexes that incur multiple roundtrips during search on remote storage (§2.3.2).

Low Rate Limits. Cloud providers often limit GET request frequency issued to each prefix (i.e., each index), ranging from 5,500 (S3 [6]) to 20,000 (Azure [54] and TOS [15]) queries-per-second (QPS) [72]. This limit is lower than typical modern SSDs (>100K [64]), and acts as a second limit to on-cloud search throughput alongside bandwidth, especially in high-concurrency settings with smaller data scales (empirically observed in §5.2). While this can potentially be addressed by caching hot index segments with local resources, current providers only cache index *metadata* [77], leading to missed opportunities; we explore integrating generalized and vector index-specific caching strategies into cloud-native vector search in §4.

2.3 On-Cloud Search Costs: Dominated by I/O

This section describes search cost models of two common vector index classes—cluster and graph indexes, and how constrained I/O of cloud environments may affect their on-cloud performance.

2.3.1 Cluster Index Search Cost. Cluster indexes are based on inverted lists for text search [13, 93]: the vector dataset is K-means clustered into n *posting lists* represented by *centroids* [37]. For search, a number of posting lists (controlled by parameter $nprobe$) with centroids closest to the query vector are fetched (e.g., SPANN uses a balanced K-means tree (BKT) built on centroids), and data vectors in the posting lists are compared with the query vector to find top- k results. Cost can be modeled for an index C as follows:

$$C_{cluster}(C) = c_{centroid}(n, nprobe) + c_{fetch}(l) + l * c_{dist} \quad (1)$$

Where $c_{centroid}(n, nprobe)$ is the cost of finding the top $nprobe$ -out-of- n posting lists, $c_{fetch}(l)$ is the cost of fetching l total vectors in the posting lists from storage, and $l * c_{dist}$ is the cost for l distance computations with the query vector. Cluster indexes features no dependencies between posting list fetches, which is a major advantage given the long roundtrips to remote storage (§2.2): resource-allowing, all $nprobe$ posting lists can be fetched at once.

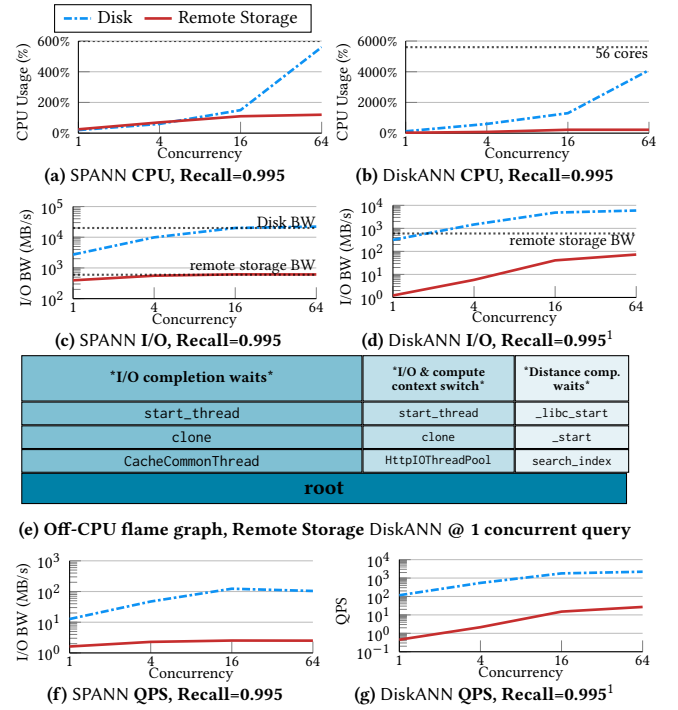


Figure 3: CPU, I/O usage, and QPS of on-disk vs. on-remote storage querying of SPANN and DiskANN on GIST1M. While search may be bottlenecked by CPU on-disk, bottlenecks are almost always network-related for cloud-native search.

Cluster Indexes’ Throughput Bottleneck. Higher query recalls demand higher $nprobe$ values, which linearly increases $c_{fetch}(l)$ and $l * c_{dist}$, while $c_{centroid}(n, nprobe)$ often becomes increasingly negligible (e.g., SPANN’s BKT trees have $O(n \log(nprobe))$ scaling [75]). Hence, cluster indexes’ performance is limited by which of I/O (for $c_{fetch}(l)$) or compute’s (for $l * c_{dist}$) bottleneck is reached first: We show via SPANN, a commonly-used cluster index, has on-cloud search costs that are dominated by the former (Fig 2a), which is also the bottleneck for its cloud-native vector search performance as we observe in Fig 2a. This bottleneck is especially prominent under high query concurrencies and recalls (Fig 3c): for example, SPANN, reading large amounts of data per query at high recalls [17] (empirically verified in Fig 8a where SPANN reads 256MB data per 0.995 recall GIST1M query), when combined with high query concurrencies, is bottlenecked by *data not arriving frequently enough* (Fig 3c) while compute is underutilized (Fig 3a). Hence, reducing data read is a key optimization point for cluster indexes’ on-cloud performance, which we study in §3.

2.3.2 Graph Index Search Cost. Graph indexes are based on KNN graphs, with each data vector connected to at most K close neighbors [26, 36, 48].² Search is performed via iterative graph traversals from *entry points* while maintaining a candidate set of current closest neighbors (with size bounded by $search_len$); then, top- k results are retrieved from the candidate set post-traversal (alg. 1).

¹DiskANN approaches the IOPS-bound at concurrency=64, which we study in §5.3.

²Different notations are used for indegree limit K , e.g., DiskANN’s R and HNSW’s M .

Algorithm 1: Graph-based iterative search for ANN

```

1 Input: query vector  $q$ , entry points  $ep$ , result size  $k$ , cand. set size  $search\_len$ 
2 Output:  $k$  closest vectors to  $q$ 
3 Initialize visited set  $V = \emptyset$ , candidate set  $C = ep$ ;
4 while  $C \setminus V \neq \emptyset$  do
5    $c \leftarrow$  extract nearest vector in  $C$  to  $q$ 
6    $C \leftarrow C \cup neighborhood(c)$ 
7    $R \rightarrow R \cup \{c\}$ 
8   if  $|C| > search\_len$ :
9     | update  $C$  to keep  $search\_len$  closest points to  $q$ 
10 Return  $k$  closest points to  $q$  in  $C$ .

```

While current graph indexes often feature some unique optimizations (e.g., HNSW’s multi-layer structure [48] and DiskANN’s extracting multiple vectors at once from the candidate set [36]), graph search cost can be largely modeled for an index G as follows:

$$C_{graph}(G) = rt \times (TTFB + c_{fetch}(K) + K \times c_{dist}) \quad (2)$$

Where rt is the number of traversal iterations (line 4 in alg. 1), $TTFB$ (i.e., time-to-first-byte) is read latency to storage, $c_{fetch}(K)$ is cost of fetching each round’s neighborhood from storage, and $K \times c_{dist}$ is the per-round vector distance computation cost. Notably, despite parallelizable data reads and distance computations in each round, the rt expansion rounds must be performed iteratively; that is, even if bandwidth and compute were *unlimited*, search still at minimum incurs $rt \times TTFB$ cost for communicating with storage.

Graph Indexes’ Read Latency Bottleneck. Higher query recalls demand the usage of larger candidate set sizes, which incurs more roundtrips, especially noticeable for high-recall queries (§2.2). Even for on-disk search, prior studies have observed that graph indexes’ search latencies are dominated by these incurred roundtrip times [80]. Accordingly, for DiskANN, a commonly-used graph index, we observe in Fig 2b that I/O% (i.e., $TTFB$) plays an even larger role in query latency due to remote storages’ longer read latencies (§2.2): for example, ad-hoc querying with DiskANN,³ which requires long, iterative traversals for high recalls [36] (empirically verified in Fig 8b where DiskANN performs 43 roundtrips per 0.995 recall GIST1M query), is bottlenecked by *waiting for data* (Fig 3e) while *both* compute (Fig 3b) and I/O bandwidth (Fig 3d) are underutilized. Hence, reducing roundtrips is a key optimization point for graph indexes’ on-cloud performance, which we study in §3.

RQ1: What Index for What Scenario? Given the bottlenecks that we have formulated and observed for two commonly-used cluster and graph indexes, SPANN and DiskANN, we can hypothesize that one reason cloud providers opt for cluster indexes is because their respective bottleneck—read throughout, degrades less from local disk to remote storage versus graph indexes’ read latency (10-20× versus ~150×), leading to lower performance drops (Fig 3f). Yet, our observations also hint at cases where graph indexes may outperform cluster indexes: for example, in Fig 3g, individual queries’ underutilization of I/O bandwidth leads to its performance scaling remarkably well w.r.t. query concurrency; we perform a detailed study of *when should graph indexes be used over cluster indexes for cloud-native search, and vice versa?* in §5.2.

³High-concurrency DiskANN workloads can also be bottlenecked by IOPS (§5.3).

(a) **Most significant overhead categories of SPANN indexing configurations on the GIST1M dataset with nprobe=640 and concurrency=1.**

Index	I/O%	Distance Comps.%	BKT Tree %
SPANN (default centroid% = 16)	63.76	4.03	1.61
SPANN (centroid% = 32)	55.30	4.46	4.46

(b) **Most significant overhead categories of DiskANN indexing configurations on the GIST1M dataset with search_len=640 and concurrency=1.**

Index	I/O%	Memory Ops. %	PQ Distance Comps.%
DiskANN (default R=64)	80.00	10.00	10.00
DiskANN (R=256)	71.42	14.29	14.29

Figure 4: Overheads of on-cloud SPANN and DiskANN. Indexes can be tuned to reduce I/O for more computations.

3 INDEX DESIGN FOR CLOUD STORAGE

As we have shown both empirically and via cost modeling in §2, two common vector index classes, cluster and graph indexes, are bound by different aspects of I/O on remote storage. This section presents some potential solutions to tuning these indexes better on-cloud performance.

Reducing Cluster Indexes’ Data Read Per Query. One of SPANN’s main optimizations for reducing data read per query is to duplicate boundary vectors (i.e., vectors with similar distance to multiple centroids) up to a user-specified `num_replica` times. While this increases individual posting list (and overall index) sizes (by up to 3× versus IVF [93], §5.3), it reduces the `nprobe` value to reach target recalls, and is often a net reduction in total data read and distance computations [17]. This optimization, along with SPANN’s increased size being a minor factor due to cheap remote storage costs (§2.1), has lead it to be TurboPuffer’s index of choice [66].⁴

Orthogonal to replication, we can increase centroid count (n in eq. (1)) to build an index with more posting lists each containing fewer vectors. Doing so would trade more distance computations for less I/O (Fig 4a); while this is discouraged for on-disk use due to both increasing BKT tree search costs [17] and index sizes (Table 4), such an index can improve on-cloud search performance where the former is dominated by $c_{fetch}(l)$ (verified in §5.3).

Reducing Graph Indexes’ Roundtrip Count. DiskANN utilizes the technique of extracting multiple vectors (controlled by `beamwidth W` [21]) at once from the candidate set per expansion round (§2.3.2),⁵ effectively performing branching traversal for each roundtrip as opposed to point-at-a-time of prior memory-based indexes’ (line 5 in alg. 1, e.g., HNSW [48] and NSG [26]). This trades more total I/O calls per query for lower roundtrip count, and is often set to a moderate value (e.g., 4-16 [21]) to balance read latency and IOPS limits (§2.2) of the environment and workload characteristics, and should be carefully tuned: using a high W value can degrade search by reaching the IOPS limit first (observed in Fig 19f).

Alternatively, to avoid increasing *any* I/O-related metrics, a denser graph with higher K in (eq. (2)) can be used, which instead trades more distance computations and larger graph size for fewer I/O calls per query *and* roundtrips. Like fine-grained cluster indexes, while dense graphs are discouraged on disk, they can often lead to performance gains for on-cloud search (Fig 4b) due to distance computations being relatively significant (verified in §5.3).

⁴TurboPuffer uses SPFresh [85], an in-place updatable extension of SPANN.

⁵Each iteration is not guaranteed to branch into the full W points, e.g., when there are fewer than W unvisited nodes in the candidate set [36, 92].

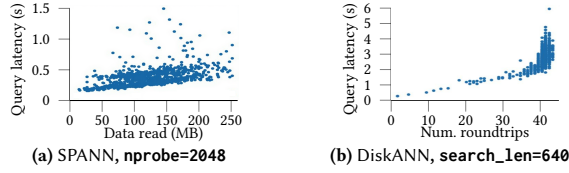


Figure 5: SPANN and DiskANN queries on GIST1M with 4GB SLRU cache; setup described in §5.1. Queries’ latencies are correlated with data read and number of roundtrips, respectively, which cache hits can help reduce.

(RQ2) How to build indexes? Through our cost modeling in terms of cluster and graph (specifically, SPANN and DiskANN) indexes’ parameters, we have identified how notable parameters can be adjusted to control the trade-offs between costs (e.g., I/O, compute). We perform benchmarking to find *How should cluster and graph indexes be built and used for optimal on-cloud performance?* in §5.3.

4 ON-CLOUD INDEX-CACHE INTEGRATION

Existing cloud-native search providers cache index metadata with local memory and SSD resources on compute: specifically, TurboPuffer caches the BKT tree of commonly-accessed SPANN indexes (§2). Doing so does benefit queries on those indexes, and has also been explored in prior on-disk works such as DiskANN and IVFPQ [60]’s in-memory caching of product-quantized dataset and codebook, respectively. Yet, following our bottleneck analyses in §2.3, the currently unexplored approach of additionally caching index data may bring further gains: this section explores existing caching works for cloud native vector search (§4.1), and discuss integration of caching and vector index optimizations in (§4.2).

4.1 Caching Benefits Vector Search

Works and surveys have found vector search workloads in production to exhibit *commonality* and *stability* patterns in production scenarios [47, 62, 63, 91], where the access patterns of posting lists of cluster-based indexes [62] and nodes of graph-based indexes [91] are both long-tailed and stable over time. These patterns have lead to effective caching solutions for related analytical tasks [40, 71], and has motivated recent studies of caching for vector search [39, 91].

Caching Index Segments. Existing caching for vector search works using well-established caching strategies: for example, GoVector [91] and CrackingIVF [47] uses an LRU cache to hold frequently visited nodes of the DiskANN index and IVF posting lists, respectively. Like many prior caching works, these works aim to maximize the cache hit rate of query workloads, and have shown via experimentation that higher cache hit rate within a query (e.g., more nodes fetched from cache) *in general* leads to lower query latency [91].

Caching to Address Cloud Bottlenecks. Accordingly, we preliminarily study of the effectiveness of these caching strategies for cloud-native vector search, by performing a cold run of GIST1M’s 1,000 queries sequentially under a high-recall (0.995), hence I/O constrained, scenario with SPANN (Fig 5a) and DiskANN (Fig 5b), using a 4GB SLRU cache (details in §5.1) to hold hot posting lists and index blocks, respectively. We expectedly observe that caching can benefit on-cloud search: cache hits for SPANN and DiskANN

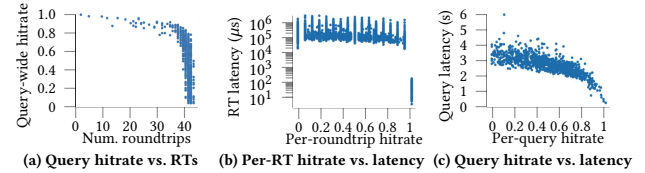


Figure 6: DiskANN: Query cache hit rate versus latencies with 4GB cache and beamwidth=16 on GIST1M. Large beamwidths decreases caching gains: all nodes visited during a round of beam search need to be cached for a roundtrip to be saved.

queries may reduce the data read and roundtrip count of individual queries, which, dominating the indexes’ cost models under high-recall settings (§2.3), would accordingly decrease query latency. However, these plots also contain peculiar patterns: while the distribution of data read per query is more uniform for SPANN (Fig 5a), the majority of queries receive few benefits from caching for DiskANN (Fig 5b), which the next section will explore (§4.2).

4.2 Index Optimizations May Harm Caching

Optimizations for on-disk indexes such as SPANN’s vector replication and DiskANN’s multi-width beam search (§3) are largely orthogonal to caching for vector search. Yet, the two may interact in surprising ways, which this section will overview.

Multi-Width Beam Search Decreases Caching Gains. We expand upon Fig 5b and study the cache hit rate metrics of GIST1M’s workload run with DiskANN in Fig 6. We can observe a noticeable non-linear relationship between query-wide hitrate (i.e., % of nodes/index blocks that were fetched from the cache during traversal) and number of performed roundtrips: the number of roundtrips to remote storage only significantly drops when cache hit rate is very high (>0.9). This is because DiskANN’s multi-width beam search ($W = 16$ in this case) *actively diminish* caching gains under non-IOPS saturated scenarios:⁶ *all* W candidates of an expansion round must be cached to save a roundtrip to remote storage (Fig 6b), which, the larger W is, the less likely this would happen and the fewer gains under the same cache size (verified in §5.4). Consequently, we observe the same non-linear relationship between query-wide hitrate and latency (Fig 6c).

(RQ3) How to utilize caching? Other negative examples between vector index optimizations and caching exist, for example, SPANN’s vector replication increasing posting list size and consequently decreasing cache hit rate under the same cache size. Hence, it is clear that optimal index parameterization for cloud-native vector search depends on available local cache size, a specific example being whether large DiskANN W values should still be used *despite* reductions in caching gains. This leads us to study the question *How should caching be utilized for on-cloud search, and how would caching also affect optimal index parameterization?* in §5.4.

5 EXPERIMENTS

This section empirically studies our proposed research questions on cloud-native vector search. We structure our study as follows:

⁶we explore this scenario in §5.4.

Table 2: Summary of Datasets for Evaluation.

Dataset	# Vectors	Dim	Data Type	# Queries	Modality
GIST1M [4]	1000000	960	FLOAT32	1000	Image
DEEP10M [8]	10000000	96	INT8	10000	Image
MSSPACE10M [78]	10000000	100	FLOAT32	30000	Document
BIGANN1B [9]	10000000	128	INT8	10000	Image

Table 3: Summary of Default Indexing/Search Parameters for Evaluation on each Dataset Unless Otherwise Stated.

Index	DiskANN			SPANN	
Dataset	PQ dim.	M	Beamwidth	centroid%	replica#
GIST1M [4]	112	64	16	16	8
DEEP10M [8]	48	64	16	12	8
MSSPACE10M [78]	112	64	16	12	8
BIGANN1B [9]	112	64	16	12	8

- (1) **Factors Affecting Cloud Indexes (§5.2):** We compare performance and bottlenecks of cluster and graph indexes on datasets and workloads with varying data dimension, concurrencies, etc., to find which scenarios each index class is performant on.
- (2) **Index Design for Cloud Storage (§5.3):** We observe how index classes' build and query parameterizations affect performance trade-offs on cloud storage—e.g., data read, computations, to provide recommendations on how to tune the indexes according to specific workload and environment characteristics.
- (3) **On-Cloud Index-Cache Integration (§5.4):** We explore gains achieved by integrating existing caching strategies applicable to caching index segments—e.g., how cache hits benefit query performance, to gain insights on how to coordinate index design and cache characteristics for maximum gains.

5.1 Experiment setup

Datasets. We use 4 experiment datasets (Table 2): GIST1M and DEEP10M are from the ANN benchmark [25]; MSSPACE10M and BIGANN1B are from the Neurips’21 BigANN benchmark [9]. We search for $k = 10$ nearest neighbors for each query in each dataset.

Methods. We study the following indexes as the representatives from their respective index classes (parameterizations in Table 3):

- **DiskANN** [36] is the state-of-the-art on-disk graph-based index. Unless stated (e.g., §5.3), we use $L = 128$, $R = 64$, $W = 16$, $sector_len = 4KB$, and $QD = \max(\frac{dim}{8}, 48)$ across all datasets.
- **SPANN** [17] is the state-of-the-art on-disk cluster-based index. Unless stated (e.g., §5.3), we use the more performant out of $centroid\% = [12, 16]$ and $num_replica = 8$ across all datasets.

System setup. We perform all experiments on a ByteDance ecs.s2-c1m4.14xlarge machine with 56 vCPUs, 224GB RAM and 100GB NIC bandwidth. We use the Volcano Engine TOS [14] for our remote storage. We build our indexes on local disk, which we then upload to remote storage. We utilize external network to access the remote storage, which has a download network bandwidth to our machine of 5Gbps, a GET request limit of 20,000QPS, and a p50 read latency of 31,000 microseconds (Table 1). For caching experiments in §5.4, we use a ByteDance in-house in-memory cache which features asynchronous data reads and writes to and from the cache [16].

We cache posting lists (for SPANN) and (4KB) index blocks (for DiskANN) following a scan-resistant LRU eviction policy [50].

Query Serving. We load the relevant index metadata into memory, i.e., BKT trees for SPANN and PQ dataset for DiskANN prior to serving each query workload on each dataset following current local caching implementations in cloud-native vector search (§4). Then we sweep $search_len \in [10, 1280]$ in power of 2 increments for DiskANN and $nprobe \in [8, 16384]$ in power of 2 increments for SPANN to generate QPS-recall curves, early stopping if the current parameterization value achieves a recall > 0.995 . We also sweep number of concurrently served queries from 1 to 64 for certain scenarios, which we control via queueing.

Measurement. At the workload level, we measure the ① *throughput* as queries-per-second (QPS) of query serving, ② *latency* (at different percentiles) as time to serve each query, and ③ average network bandwidth,⁷. For index-specific metrics, we measure ④ *number of neighbor expansions* performed for each DiskANN query and the ⑤ *number of visited posting lists* for each SPANN query. For query-specific metrics, we measure ⑥ *per-request mean I/O latency* of individual SPANN posting lists and DiskANN per-expansion node batches,⁸ and ⑦ *cache hit rate* for settings with a cache.

Reproducibility. Our benchmarking scripts and datasets are open-sourced in our Github Repository [10].

5.2 What Index For What Scenario?

This section studies the comparison between DiskANN and SPANN indexes on remote storage. We build the two indexes for each dataset following procedures described in §5.1, then study the metrics and performance of each index on different query workloads.

We report results in Fig 7. We can observe that DiskANN outperforms SPANN in high-concurrency and/or recall scenarios on all datasets, matching observations in prior studies for on-disk indexing [18, 69]. Focusing on results on GIST1M (Fig 7e), we can see that the cutoff is at ~ 0.8 recall with 16 concurrent queries (Fig 7c); SPANN outperforms DiskANN at all recalls at lower concurrencies (Fig 7a, Fig 7b), and vice versa at higher concurrencies (Fig 7d).

The detailed query metrics in Fig 8 and mean I/O latencies in Fig 9 hint at the reasons: each SPANN query reads a large amount of data, from 2.5MB at 0.7 recall to 256MB at 0.995 recall, which is 9.39 \times and 94.8 \times more than DiskANN at the same recalls, respectively (Fig 8a). Hence, SPANN exhibits significant I/O congestion at high recalls (Fig 9a) and concurrencies (Fig 9b) as these two settings both contend for I/O bandwidth (§2.2) due to the index’s concurrent queuing—both inter and intra-query (§2.3.1)—of posting lists: at 0.995 recall and 64 concurrent queries, SPANN’s posting list mean I/O latency is *21.6 seconds*, and the bandwidth is only enough to serve 2.5 SPANN queries per second at this recall. Conversely, DiskANN’s exhibits significantly less I/O congestion—its batched node expansion requests having 416 \times lower mean I/O latency versus SPANN at 0.995 recall and 64 concurrent queries, due to its iterative traversal spreading out its (already low) data requests to exhibit consistent bandwidth utilization at different recalls (Fig 3d).

⁷Computed as total data read/real elapsed workload time.

⁸Implementation-wise, SPANN issues separate requests for posting lists [59], while DiskANN batches the W requests of each expansion [55]. On the remote storage side, DiskANN’s W batched requests will still count as W IOs for IOPS throttling [14].

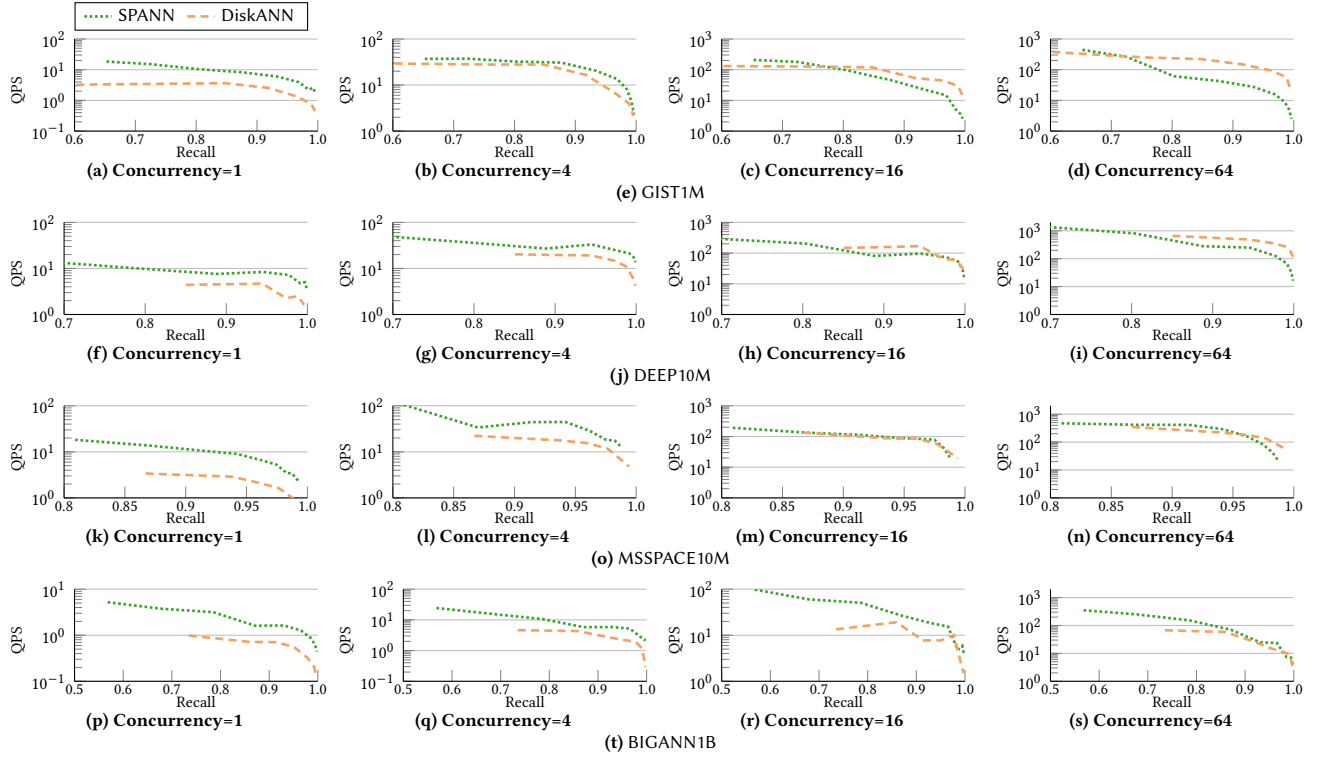


Figure 7: QPS-recall curve of SPANN versus DiskANN at different query concurrencies on GIST1M. DiskANN outperforms SPANN at high query recalls and concurrencies and vice versa.

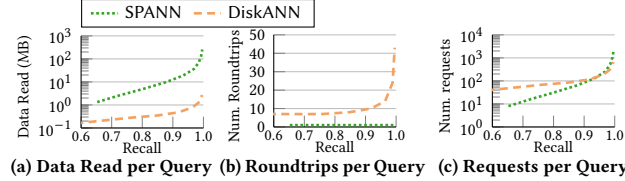


Figure 8: Query metrics of SPANN and DiskANN on GIST1M. SPANN reads significantly more data per query versus DiskANN, but DiskANN’s requests are spread across roundtrips due to dependencies within graph traversal (§2.3).

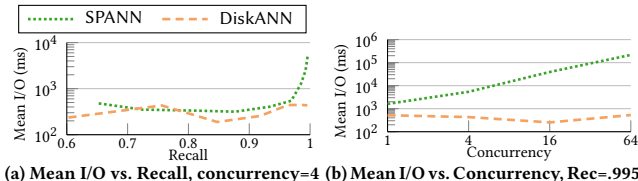


Figure 9: Mean I/O of on-disk vs. on-remote storage querying of SPANN on GIST1M. SPANN exhibits notable I/O congestion at both high recalls and concurrencies.

Yet, the disadvantage of DiskANN’s iterative traversal becomes apparent under lower concurrency settings: it makes multiple roundtrips per query due to its iterative traversal, from 7 at 0.7 recall to 43 at 0.995 recall (Fig 8b). DiskANN queries have a latency of 285 ms when sequentially running queries at 0.7 recall (Fig 7a), where if we follow the read latencies observed in Table 1, suggests that on average 217 ms was spent on communicating with remote storage alone.

Inability to fully utilize I/O bandwidth for individual queries unlike SPANN’s concurrent fetching of posting lists leads to DiskANN having 5.71 \times higher versus SPANN at this setting.

Finally, despite DiskANN reading less data per query versus SPANN at all recalls, DiskANN makes more requests per query at low recalls (Fig 8c): at 0.7 recall, each DiskANN query averages at 38.4 requests while SPANN averages at 7.9 requests; SPANN overtakes DiskANN at 0.995 recall with 2003.6 and 660.0 requests, respectively. This matches conventional wisdom for the indexes’ performance for on-disk querying [30], where DiskANN is outperformed by SPANN at low recalls and vice versa, due to SSD performance being comparatively more sensitive to DiskANN’s large number of random (4KB) reads at low recalls. For cloud-native vector search, requests per query affects when each index will potentially be bottlenecked by IOPS limits, which we can observe in a variety of settings shortly (e.g., Fig 10c).

DEEP10M: Low-Dimension Datasets Benefit SPANN. DEEP10M features 96D vectors instead of GIST1M’s 960D vectors (Table 2), and also a higher recall/concurrency cutoff for DiskANN to outperform SPANN at 0.99 recall with 16 concurrent queries (Fig 7h). These two factors are related: SPANN benefits two-fold from querying on a low-dimension dataset (Fig 10): the same recall can be reached with a lower nprobe value, with only nprobe=512 required to reach 0.995 recall on DEEP10M versus GIST1M’s 2048 (Fig 10a, also empirically verified by Milvus [61]), and each posting list, containing the same number of significantly lower-dimension vectors,⁹

⁹Recall that SPANN uses a percentage of points as centroids.

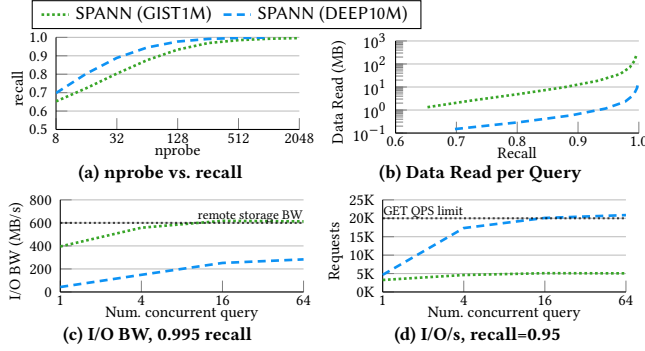


Figure 10: SPANN on DEEP10M: lower-dimension dataset reduces posting list size and nprobe values required to reach certain recalls. This significantly reduces data read per query and improves QPS at high recalls and concurrencies, but querying may still be bound by remote storage IOPS.

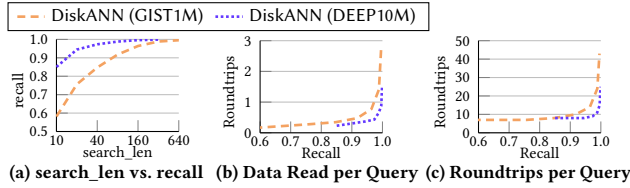


Figure 11: DiskANN on DEEP10M: lower-dimension dataset reduces search_len values for certain recalls and consequently roundtrips, which DiskANN’s QPS benefits (one-fold) from.

are significantly smaller—15.0KB on DEEP10M versus 166KB on GIST1M. These two factors combined significantly reduce the data read per query at the same recall by up to 28.4x (Fig 10b) and consequently improve QPS by up to 7.61x at 0.995 recall (concurrency=4, Fig 7g). Notably, despite the reduction in data read, SPANN’s QPS on DEEP10M is still bottlenecked by remote storage’s GET QPS at high recalls and concurrencies (Fig 10d): despite the I/O bandwidth only being at 283 MB/s at concurrency=64 and 0.995 recall (Fig 10c), the QPS improves by only 1.12x from concurrency=16 to 64 (Fig 7j).

In contrast, DiskANN benefits only one-fold from querying on DEEP10M; while the same recall can similarly be reached with a lower search_len value—160 on DEEP10M vs. 640 on GIST1M for 0.995 recall (Fig 11a), which reduces data read per query by 3.07x (Fig 11b) and roundtrips by 2.88x (43 to 15, Fig 11c) at this recall, none of these metrics further benefit from the reduced vector dimensions as DiskANN reads data in fixed 4KB blocks [55]. Hence, the QPS of DiskANN only improves by up to 2.86x at 0.995 recall from GIST1M to DEEP10M (concurrency=1, Fig 7f).

MSSPACE10M: Quantized Datasets Benefit SPANN. MSSPACE10M features 100D vectors of quantized INT8 datatype, which when compared to the similar-dimension DEEP10M using FLOAT32, has $\sim 4\times$ smaller-sized vectors (Table 2). MSSPACE10M features an even higher recall/concurrency cutoff for DiskANN to outperform SPANN at 0.96 recall and 64 concurrent queries (Fig 7n). This is because SPANN benefits from the smaller-size INT8 datatype on MSSPACE10M, reading a uniform 2.69x less data per query versus DEEP10M at every nprobe value (Fig 12a) allowing for better utilization of I/O bandwidth (Fig 12b). This significantly improves QPS

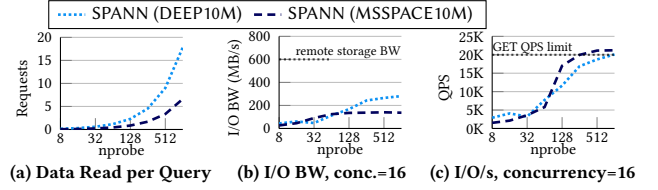


Figure 12: SPANN on MSSPACE10M: quantized datatypes (e.g., INT8) reduces posting list size and data read per query, improving QPS when the GET QPS limit is yet to be reached.

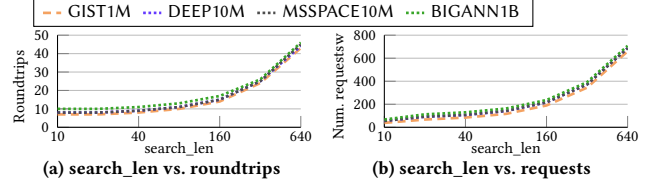


Figure 13: DiskANN’s average roundtrips and number of requests per query versus dataset size: both of these metrics scale logarithmically versus dataset size; DiskANN’s query latency is significantly correlated with the former.

at lower nprobe values (up to 2.13x at nprobe=8, Fig 7m), with the improvement diminishing as the GET QPS limit is approached (Fig 12c), down to only up to 1.05x at nprobe=1028 (Fig 7n).¹⁰ Due to fixed block read sizes, DiskANN does not benefit from quantized datatypes QPS-wise given fixed search_len values.

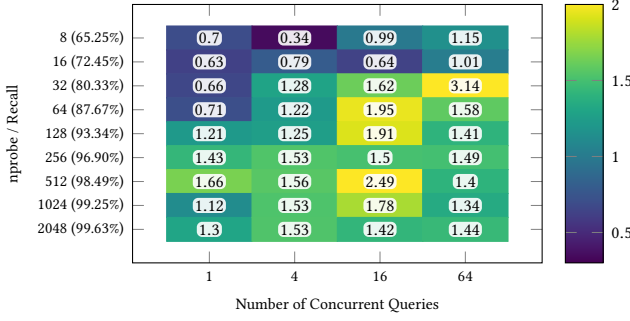
BIGANN1B: Large Datasets Benefit SPANN. BIGANN1B features 1 billion 128D INT8 vectors, and has the highest recall/concurrency cutoff for DiskANN to outperform SPANN, at 0.99 recall with 64 concurrent queries (Fig 7s). This is because while both indexes contains components that exhibit logarithmic scaling with dataset size—SPANN’s BKT tree traversal time (§2.3.1), and DiskANN’s number of roundtrips [90] (Fig 13a) and requests per query [35] (Fig 13b), SPANN’s BKT tree search is performed entirely in memory and comprises a small portion of the overall search cost (Fig 2a), while DiskANN’s metrics, especially number of roundtrips, is core to the query latency (Fig 5b).

A1: What index for what scenario? In general, SPANN features lower query latency versus DiskANN, at the cost of higher data read per query, and more I/Os per query at high recalls. Consequently, under typical cloud setups, DiskANN outperforms SPANN at high query recalls and/or concurrencies and vice versa. Dataset characteristics will affect balance: low vector dataset dimensionality, small (e.g., quantized) datatypes, and larger dataset size shift the balance in favor of SPANN.

5.3 How to Design Indexes?

This section studies how SPANN and DiskANN can be adjusted for cloud-native vector search. We explore how various parameterizations, even those outside the recommended range for on-disk

¹⁰Different datasets achieve different recalls with different nprobe values. We use nprobe vs. QPS to isolate the effect of datatype.



(a) Ratio of (centroid% = 32 QPS/centroid% = 16 QPS) of SPANN on GIST1M

Figure 14: QPS ratio of the alternative SPANN index with fine-grained posting lists (centroid% = 32) over the default centroid% = 16 index. The alternative achieves significant QPS increases on high recall and/or concurrency scenarios.

Table 4: Size metrics of SPANN configurations on GIST1M.

Configuration	Index size (GB)	No. lists	Avg. list size (KB)
SPANN (centroid% = 16, replica = 8)	13.0	159K	166
SPANN (centroid% = 16, replica = 4)	10.5	159K	138
SPANN (centroid% = 16, replica = 2)	7.5	159K	99
SPANN (centroid% = 32, replica = 8)	14.0	271K	119

querying, may achieve higher on-cloud query performance according to our cost models (§3) on the GIST1M dataset.

SPANN: More Centroids Benefit I/O-Congested Setups. Fig 14 reports the QPS ratio of an alternative SPANN index built with a higher centroid% = 32 versus the default SPANN index built with centroid% = 16. As hypothesized in §3, the former achieves QPS gains versus the latter on high recall and/or concurrency scenarios (up to 3.14×) as the centroid% = 32 count index contains more posting lists each of significantly smaller size (by 32.1%, Table 4),¹¹ which significantly reduces the amount of data read per query (1.47× at 0.995 recall, Fig 15a). The network metrics at 0.995 recall affirm this: while bandwidth is still saturated (Fig 15b), the mean I/O latency has decreased by 1.39× at 0.995 recall with concurrency = 64 (Fig 15c).¹²

However, the centroid% = 32 index underperforms versus the centroid% = 16 index on low concurrency and/or recall scenarios where the I/O congestion is low (Fig 9). As previously shown in Fig 4a, despite saving I/O costs, the centroid% = 32 index incurs higher distance computations and BKT Tree traversal costs, losing performance when BKT tree search overhead ($O(\log n)$) is more significant than that of I/O cost ($O(n)$), matching conventional wisdom of using centroid counts of under 20% for on-disk querying [17].

SPANN: Replication Count Impacts Index Quality. Another method for reducing SPANN’s posting list sizes without increasing posting list count (i.e., BKT tree costs) is to decrease vector replication. We test two SPANN indexes with reduced vector replication counts of 4 and 2 in Fig 16: Despite data read per query being reduced at various nprobe values due to smaller posting list sizes (Table 4), these indexes do not necessarily result in better

¹¹SPANN contains optimizations for pruning redundant centroids [17], hence the actual number of centroids is less than 32%.

¹²For each nprobe value, the centroid% = 32 achieves similar recalls versus the centroid% = 16 index ($\pm 1\%$). We treat them as identical for brevity.

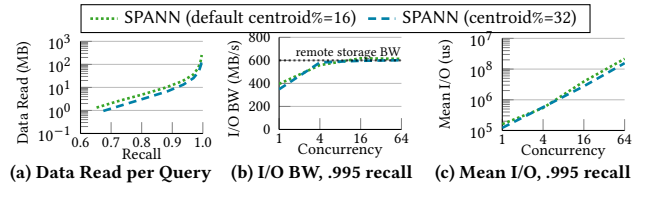


Figure 15: SPANN on GIST1M: Increasing the number of centroids and consequentially decreasing posting list size significantly reduces data read per query (left). While bandwidth is still saturated on high recall/concurrency scenarios (middle), congestion is significantly reduced (right).

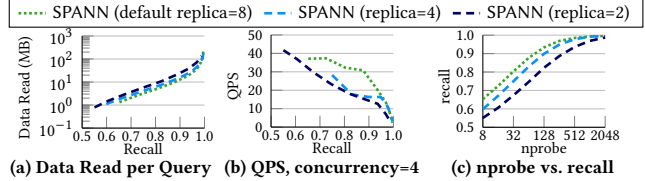
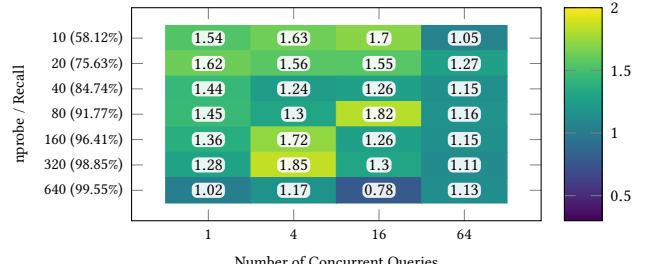


Figure 16: SPANN on GIST1M: reducing replication decreases posting list size, but does not necessarily reduce data read per query at the same recall (left) and can negatively impact QPS-recall trade-off (middle) due to lower-quality indexing requiring higher nprobe values to reach the same recall (right).



(a) Ratio of (R=256 QPS/R=64 QPS) of DiskANN on GIST1M

Figure 17: QPS ratio of the alternative DiskANN index with denser graph (R=256) over the default graph with R=64. The denser graph achieves consistent QPS increases across all recalls and concurrencies on remote storage.

QPS-recall trade-offs: reducing replication count also reduces index quality, which results in a higher nprobe value required to reach the same recall—for example, the replica = 2 index requires 3–4× higher nprobe versus the replica = 8 index to reach the same recall at all recall levels (Fig 16c), ultimately resulting in *more* data read per query at the same recall (Fig 16a) and lower QPS (e.g., 2.00× more data read and 1.92× lower QPS vs. replica = 8 @ 0.97 recall).

DiskANN: Denser Graphs Benefit Cloud Setups. Fig 17 reports the QPS ratio of an alternative DiskANN index built with a higher density (R = 256) versus the default DiskANN index built with R = 64. While having a larger size (8.2GB vs. 7.1GB), the former achieves consistent (up to 1.85×) QPS gains versus the latter on all scenarios. The detailed metrics in Fig 18 showcase reasons: the R = 256 graph reduces the number of roundtrips to remote storage (Fig 18a) and the number of requests per query (Fig 18b) at all recalls, which address DiskANN’s I/O bottleneck (Fig 4b) to improve query performance.

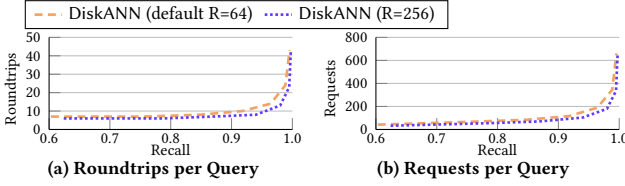


Figure 18: DiskANN on GIST1M: a denser graph reduces the number of roundtrips and requests to storage per query, benefitting on-cloud performance.

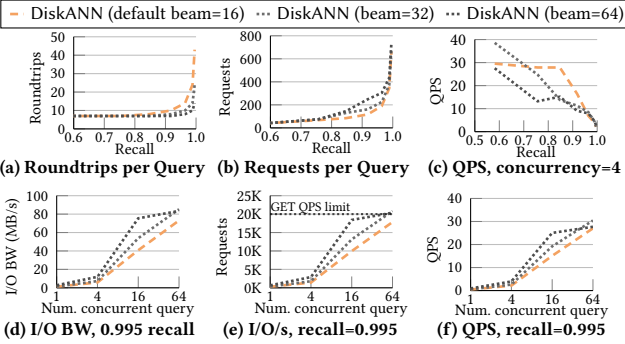


Figure 19: DiskANN: higher beamwidth can reduce roundtrips while increasing requests per query. This only improves QPS at low concurrency and high recalls (top); it reduces QPS at high concurrencies from saturating IOPS limit (bottom).

DiskANN: High Beamwidth for High Recall Ad-Hoc Queries. Alternatively, a higher search beamwidth may also reduce the number of roundtrips per query, which we study in Fig 19. Fig 19a shows that there are only significant reductions at high recalls, from 43 to 14 at 0.995 recall, which consequently improves QPS by 1.85× with concurrency=4 (Fig 19c). However, higher beamwidths incur more requests per query (Fig 19e), which decreases QPS under all other scenarios: each query still incurs 7 roundtrips regardless of beamwidth at 0.8 recall, leading to a 1.83× QPS decrease in correspondance to the 1.71× request increase from beamwidth=16 to 64. On the other hand, higher beamwidths saturates the IOPS limit more easily at high concurrencies: while I/O bandwidth to remote storage is far from saturated with beamwidth=64 even at concurrency=64 (83.4 MB/s, Fig 19d), the 20K IOPS limit has been reached even with beamwidth=32 (Fig 19e), resulting in beamwidth=32 having 1.10× QPS versus beamwidth=64 at concurrency=64 (Fig 19f).

A2: How to design indexes? SPANN and DiskANN both have parameters which can address their specific bottlenecks for cloud-native vector search: For SPANN, this would be using more centroids for high recall/concurrency scenarios to trade lower data read per query for BKT tree computations; for DiskANN, this would be using a denser graph to trade fewer roundtrips for more distance computations, while selectively using higher beamwidth for high-recall setups to further reduce roundtrips when the concurrency is sufficiently low such that the higher requests per query does not saturate IOPS limit.

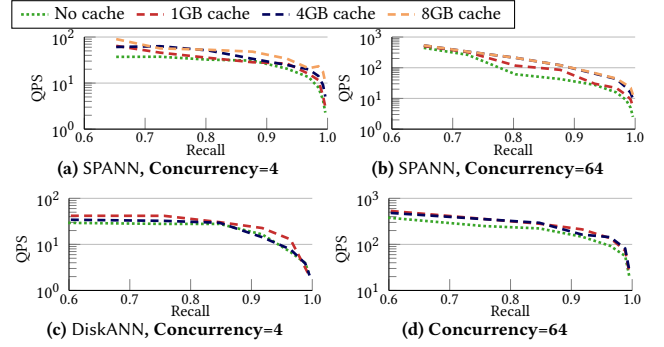


Figure 20: QPS-recall curve of SPANN and DiskANN with various cache sizes and concurrencies on GIST1M. SPANN benefits from a larger-sized cache; DiskANN gains no notable benefits from increasing cache size beyond a small threshold (1GB) under non IOPS-saturated settings.

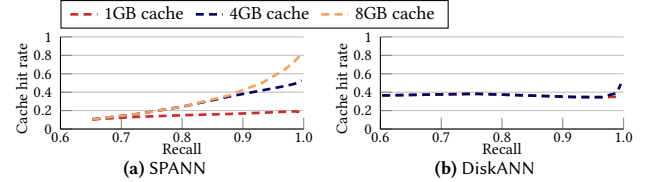


Figure 21: Cache hit rate versus size of SPANN and DiskANN on GIST1M, which both exhibit higher hit rate at higher recalls.

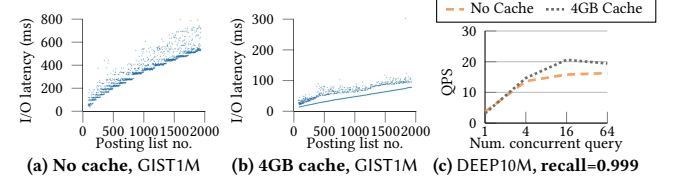


Figure 22: SPANN: cache hits benefits an example query on GIST1M by reducing bandwidth pressure induced by concurrent posting list fetching (left, middle). It is similarly effective at IOPS pressure, which we observe on DEEP10M (right).

5.4 How to Utilize Caching?

This section studies how to effectively utilize local caching for index segments in cloud-native vector search. We evaluate caching gains with various cache sizes set up following §5.1, and investigate performance gains and metrics under different index parameterizations and datasets to understand how to effectively utilize caching for on-remote storage querying. We perform all experiments with a cold start, i.e., empty cache, in this section. We report caching gains on GIST1M in Fig 20,¹³ and hitrate versus recall in Fig 21.

SPANN: Cache Hits saves Network Resources. SPANN benefits more from caching at high concurrencies, larger cache sizes, and higher recalls. The first two factors are straightforward: SPANN exhibits more I/O congestion at high concurrencies which caching addresses, and a larger cache holds more posting lists for higher hit rate (Fig 21a), which is especially noticeable at high recalls: SPANN's

¹³All 1K queries on GIST1M read less than 4GB data combined with DiskANN, making 4GB and 8GB caches functionally identical. We omit the latter from the plot for brevity.

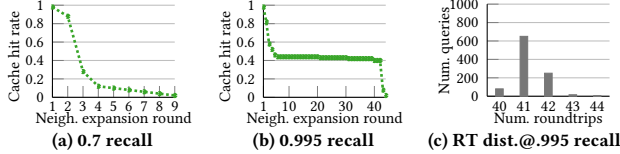


Figure 23: DiskANN’s per-neighbor expansion round cache hitrate: the first few rounds corresponding to expanding around the graph’s entry point exhibits the highest hitrates regardless of query parameterization.

large amount of data read per query at high recalls (Fig 8a) leads to high cache locality, with queries reading more overlapping posting lists; this leads to the 1GB cache being insufficient for holding all ‘hot’ posting lists: while the 4GB cache’s hit rate reaches 0.68 at 0.995 recall, the 1GB cache’s hit rate in fact drops from 0.19 to 0.17 from 0.98 to 0.995 recall, explaining the significant performance difference between the 1GB and 4GB caches at this recall (Fig 20). In particular, SPANN’s cache hits benefits both individual queries and workloads as a whole (Fig 22; for the former, it reduces the bandwidth pressure of concurrently fetching posting lists, which we observe for an example query on GIST1M where the significant queuing of posting list requests (Fig 22a) is reduced with a 4GB cache (Fig 22b)—the I/O latencies exhibit a bimodal distribution between cache hits and misses. Caching reduces the total data read and number of requests of the workload for the latter, which, in addition to addressing bandwidth congestion, similarly addresses IOPS congestion as we have observed on the DEEP10M dataset (Fig 10d) at high recalls and concurrencies (Fig 22c).

DiskANN: Cache Hits Benefit Early Expansion Latency. DiskANN receives similar benefits from the 1GB and 4GB caches under low concurrencies (up to 1.41 \times for both sizes for concurrency=4), and unlike SPANN, noticeably benefits more from caching at low recalls (1.41 \times @0.7 recall vs. 1.02 \times @0.99 recall w/ 4GB cache, Fig 20) *despite* higher cache hit rates from better cache locality due to overlapping query blocks (0.49 vs. 0.35 hitrate from 0.7 to 0.99 recall w/ 4GB cache). These factors can be attributed to DiskANN’s unique interaction between beamwidth and cache hits (§4.2): Fig 23 shows that the first few roundtrips (i.e., the DiskANN graph’s entry point neighborhood) consistently have near-1 hitrates regardless of recall: these saved initial roundtrips comprise a larger portion of traversal at low recalls (Fig 23a) versus at high recalls (Fig 23b). Interestingly, we also observe a trimodal distribution in per-expansion cache hit rate in Fig 23b, where the hit rate of the latest rounds (>42) performed by long-tailed, difficult queries (Fig 23c) are near-0, as these rounds require visiting seldomly re-visited sparse graph regions [36]. However, like SPANN, under IOPS-saturated settings (e.g., concurrency=64 and >0.99 recall), DiskANN does gain performance with larger cache size, with the 4GB cache achieving 1.45 \times QPS increase versus 1GB cache’s 1.30 \times (Fig 20d): while cache hits may still not reduce the number of roundtrips, they effectively reduce the number of requests per query and consequently IOPS.

SPANN: Reducing Replication Increases Hit Rate. One potential drawback of SPANN’s vector replication is that it increases posting list size (Table 4), which reduces the number of posting lists a fixed-size cache holds and potentially the cache hit rate

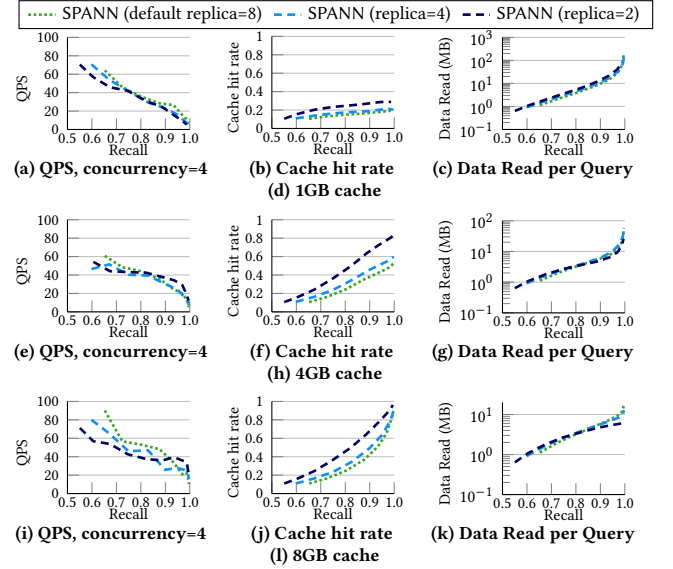


Figure 24: SPANN on GIST1M: reducing replication decreases posting list size to improve cache hit rate. This brings performance benefits to offset recall drop at fixed nprobe values given sufficiently-sized caches (e.g., 4GB); when cache is large (e.g., 8GB), replication should be increased again.

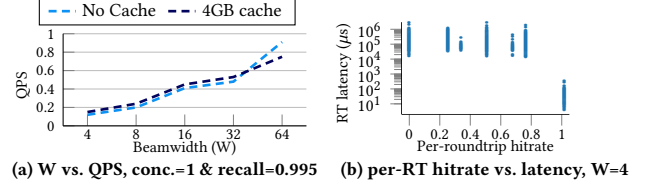


Figure 25: DiskANN on GIST1M: While larger beamwidth benefits ad-hoc querying at high recalls, it also diminishes caching gains due to decreased chances of saving roundtrips.

(§4.2). We observe this in Fig 24 where we evaluate the various low-replication SPANN indexes under various cache sizes: while low-replication indexes reduce QPS-recall trade-off without a cache (Fig 16b), when combined with a sufficiently-sized cache (i.e., 4GB), their smaller posting lists significantly increases the cache hit rate, and consequently the data read per query. For example, despite the replica=2 index requiring nprobe=1024 to reach 0.97 recall versus the replica=8 index requiring nprobe=256, it still reads 3.09 \times less data per query (Fig 24g) due to its significantly higher cache hit rate (0.778 vs. 0.467, Fig 24f), leading to a 2.03 \times QPS increase at this recall and concurrency=4 (Fig 24e). Interestingly, with smaller (e.g., 1GB, Fig 24d) or even larger (e.g., 8GB Fig 24l) cache size, replica=8 becomes optimal again: low-replication indexes do not achieve sufficiently higher cache hit rate for the former (Fig 24b), and replica=8 already has sufficiently high hitrate for the latter (Fig 24j).

DiskANN: Caching Enables Higher Beamwidth Usage. We have observed caching to bring negligible benefits to the latter roundtrips of queries due to low hitrates (Fig 23); in fact, for ad-hoc queries (i.e., concurrency=1), the higher the beamwidth, the lower the QPS benefits due to the decreased possibility of caching all nodes of a

roundtrip—for example, it is much more likely for a roundtrip to be saved via caching under $W=4$ (§4.2) versus $W=16$ (Fig 6a). However, under cases where high beamwidth is beneficial (e.g., high-recall, ad-hoc querying as shown in Fig 25a), caching benefits ($1.25\times$ at $W=4$) are insignificant versus gains from increasing beamwidth ($7.58\times$ from $W=4$ to 64), hence the latter should be used regardless.

A3: How to Utilize Caching? SPANN benefits from caching as cache hits reduce I/O bandwidth and/or IOPS pressure of concurrent posting list fetching. Benefits can be increased under moderate cache sizes (i.e., insufficient for holding enough hot posting lists under high replication) by reducing replication factor to reduce posting list size and increase cache hit rate; effectiveness of this approach diminishes when the cache is too small even when replication is reduced regardless, or when the cache is large enough.

DiskANN’s multi-node expansions result in its individual queries only significantly benefitting from caching latency-wise in its first few expansions; hence, for non IOPS-saturated settings, it may be sufficient to use a fixed-size cache which holds the neighborhood around the graph’s entry point as suggested in the original DiskANN paper [36]. A standard (e.g., LRU) cache may still be used under IOPS-saturated settings. While high beamwidth decreases caching gains due to further decreased chances of saving roundtrips, caching gains are often insignificant versus beamwidth-induced gains; beamwidth should be set following A2 (§5.3) as if there is no cache.

6 RELATED WORK

Cloud-Native Vector Search. TurboPuffer and Amazon S3 Vector have recently began offering cloud-native vector search services [12, 77]. Differing from prior providers utilizing cloud storage only to persist vector indexes and perform querying entirely in memory [5, 31], these cloud-native providers query vector indexes directly on cloud storage, fetching index segments on demand. Notably, cloud-native providers have only explored querying with cluster indexes, and only utilize local caching to hold index metadata (e.g., SPANN BKT trees, §4.1) of hot indexes. Our work complements development of these cloud-native vector search systems by identifying bottlenecks of the two index classes on remote storage, and accordingly providing suggestions on the index (and parameters) and caching strategy, to use for different workloads (§5).

Data placement for on-disk graph indexes. There exists works aimed at optimizing the node placement of on-disk graph-based indexes aiming to improve data locality [19, 42, 80, 87]. Starling [80] aims to place neighboring nodes in the same index block to reduce the total number of I/O calls performed during expansion; MARGO [87] builds on Starling to additionally place nodes on common paths into the same block aiming to perform multiple expansion rounds with one roundtrip to storage. According to our findings on bottlenecks of graph indexes when high beamwidth values are used (§5.3), these works would effectively address incurred IOPS limits to further increase throughput under high concurrency and long roundtrip times, respectively, making their integration into on-cloud vector search pipelines promising.

Quantization for cluster indexes. Some works have proposed quantization-aware optimizations for cluster indexes [28, 41, 60, 65]. A common theme is to reduce the accuracy loss incurred on the index by quantization, which techniques such as clustering on quantized distances [28, 65] and per-posting list quantization [41] aim to accomplish. Orthogonally, IVF-PQ [60] partitions vectors into segments and performs per-segment quantization and clustering. We have observed that the two key bottlenecks of on-cloud cluster indexes are the large amount of data read and I/O calls (§5.2); while quantization would reduce posting list size and improve throughput in bandwidth-constrained settings, our results suggest that quantization would be less effective when the IOPS constraint is instead reached (e.g., on low-dimension datasets such as DEEP10M, Table 2), necessitating alternative techniques such as caching.

ANN query latency reduction via early stopping. Studies have found vector ANN queries to feature varying hardness levels [3, 83], and works have accordingly proposed methods for early-stopping easy queries in both graph indexes [17, 44, 89] and cluster indexes [73, 84]. LAET [44] and Auncel [89] uses mid-query-serving features to dynamically early-stop graph traversal; SPANN [17] uses a heuristic-based method to skip posting lists with centroids far from the query vector, while Tribase [84] and TRIM [73] further use triangle inequalities to early stop within-posting list distance computations. While early stopping will improve the performance of on-cloud search with graph indexes by reducing roundtrips, our results suggest that adopting within-posting list early stopping for cluster indexes will require more consideration as these techniques aim to reduce the computations on *already fetched* data, which is often not a primary bottleneck of cluster indexes (§5.3).

Caching for Vector Indexes. GoVector [91] and CALL [38] have recently proposed methods for improving the cache hit rate of caching strategies applied to graph index blocks and cluster index posting lists, respectively. GoVector utilizes a path-aware caching strategy to prioritize keeping nodes on the same common paths, while CALL proposes a grouping strategy to improve cache locality. Specifically for graph indexes, our work has shown that higher cache hit rate does not necessarily imply lower latency for individual queries when combined with DiskANN’s beamwidth-specified multi-node expansion (§5.4), and that further developing a beamwidth-aware caching strategy would be valuable future work for on-cloud search.

7 CONCLUSION

In this paper, we present a comprehensive performance analysis for cloud-native vector search. We perform principled cost modeling for two representatives of the commonly-used graph and cluster vector index classes, SPANN and DiskANN, both theoretically and empirically show their bottlenecks in cloud-native vector search settings, and how local caching can be integrated with these indexes for performance gains. Then, we accordingly provide insights on (1) which index to use for a wide variety of workloads with different latency, throughput, recall, query concurrency, and dataset properties, (2) how to improve the performance of the chosen index via tuning its parameterization according to the workload characteristics, and (3) how indexing should be adjusted for further performance gains under various available local cache sizes.

REFERENCES

- [1] Amazon. [n.d.]. Amazon S3 - Pricing. <https://aws.amazon.com/s3/pricing/>.
- [2] Amazon. [n.d.]. Cloud Object Storage - Amazon S3. <https://aws.amazon.com/pm/serv-s3>.
- [3] Fabrizio Angiulli. 2018. On the behavior of intrinsically high-dimensional spaces: distances, direct and reverse nearest neighbors, and hubness. *Journal of Machine Learning Research* 18, 170 (2018), 1–60.
- [4] Antonia Torralba Aude Oliva. [n.d.]. Modeling the shape of the scene: a holistic representation of the spatial envelope. <http://people.csail.mit.edu/torralba/code/spatialevelope/>.
- [5] AWS. [n.d.]. Amazon OpenSearch Service's vector database capabilities explained. <https://aws.amazon.com/blogs/big-data/amazon-opensearch-services-vector-database-capabilities-explained/>.
- [6] AWS. [n.d.]. Amazon S3 Announces Increased Request Rate Performance. <https://aws.amazon.com/about-aws/whats-new/2018/07/amazon-s3-announces-increased-request-rate-performance/>.
- [7] AWS. [n.d.]. The Floodgates Are Open - Increased Network Bandwidth for EC2 Instances. <https://aws.amazon.com/blogs/aws/the-floodgates-are-open-increased-network-bandwidth-for-ec2-instances/>.
- [8] Artem Babenko and Victor Lempitsky. 2016. Efficient indexing of billion-scale datasets of deep descriptors. In *Proceedings of the IEEE Conference on Computer Vision and Pattern Recognition*. 2055–2063.
- [9] Big ANN benchmarks. [n.d.]. Billion-Scale Approximate Nearest Neighbor Search Challenge: NeurIPS'21 competition track. <https://big-ann-benchmarks.com/neurips21.html>.
- [10] BillyZhaohengLi. [n.d.]. cloud-native-vector-index. <https://github.com/BillyZhaohengLi/cloud-native-vector-index>.
- [11] Microsoft Bing. [n.d.]. Bing Visual Search. <https://developer.nvidia.com/blog/optimizing-microsoft-bing-visual-search-with-nvidia-accelerated-libraries/>.
- [12] AWS Blogs. [n.d.]. Introducing Amazon S3 Vectors: First cloud storage with native vector support at scale (preview). <https://aws.amazon.com/blogs/aws/introducing-amazon-s3-vectors-first-cloud-storage-with-native-vector-support-at-scale/>.
- [13] Eric W Brown, James P Callan, and W Bruce Croft. 1994. Fast incremental indexing for full-text information retrieval. In *VLDB*, Vol. 94. 9.
- [14] ByteDance. [n.d.]. Volcano Engine Object Storage. <https://www.volcengine.com/product/TOS>.
- [15] ByteDance. [n.d.]. Volcano Engine TOS - Bandwidth. <https://www.volcengine.com/docs/6349/74823>.
- [16] Jianjun Chen, Rui Shi, Heng Chen, Li Zhang, Ruidong Li, Wei Ding, Liya Fan, Hao Wang, Mu Xiong, Yuxiang Chen, et al. 2023. Krypton: real-time serving and analytical SQL engine at ByteDance. *Proceedings of the VLDB Endowment* 16, 12 (2023), 3528–3542.
- [17] Qi Chen, Bing Zhao, Haidong Wang, Mingqin Li, Chuanjie Liu, Zengzhong Li, Mao Yang, and Jingdong Wang. 2021. Spann: Highly-efficient billion-scale approximate nearest neighborhood search. *Advances in Neural Information Processing Systems* 34 (2021), 5199–5212.
- [18] Rongxin Cheng, Yifan Peng, Xingda Wei, Hongrui Xie, Rong Chen, Sijie Shen, and Haibo Chen. 2024. Characterizing the dilemma of performance and index size in billion-scale vector search and breaking it with second-tier memory. *arXiv preprint arXiv:2405.03267* (2024).
- [19] Benjamin Coleman, Santiago Segarra, Alexander J Smola, and Anshumali Shrivastava. 2022. Graph reordering for cache-efficient near neighbor search. *Advances in Neural Information Processing Systems* 35 (2022), 38488–38500.
- [20] Linux Perf Contributors. [n.d.]. perf: Linux profiling with performance counter. <https://perfwiki.github.io/main/>.
- [21] DiskANN. [n.d.]. DiskANN-Py - API. <https://microsoft.github.io/DiskANN/docs/python/latest/diskannpy.html>.
- [22] Dominik Durner, Viktor Leis, and Thomas Neumann. 2023. Exploiting cloud object storage for high-performance analytics. *Proceedings of the VLDB Endowment* 16, 11 (2023), 2769–2782.
- [23] eBay. [n.d.]. eBay's Blazingly Fast Billion-Scale Vector Similarity Engine. <https://innovation.ebayinc.com/stories/ebays-blazingly-fast-billion-scale-vector-similarity-engine>.
- [24] Philipp Eichmann, Emanuel Zgraggen, Carsten Binnig, and Tim Kraska. 2020. Idebench: A benchmark for interactive data exploration. In *Proceedings of the 2020 ACM SIGMOD International Conference on Management of Data*. 1555–1569.
- [25] erikbern. [n.d.]. ann-benchmark - Benchmarks of approximate nearest neighbor libraries in Python. <https://github.com/erikbern/ann-benchmarks>.
- [26] Cong Fu, Chao Xiang, Changxu Wang, and Deng Cai. 2017. Fast approximate nearest neighbor search with the navigating spreading-out graph. *arXiv preprint arXiv:1707.00143* (2017).
- [27] Frank Gadban and Julian Kunkel. 2021. Analyzing the performance of the S3 object storage API for HPC workloads. *Applied Sciences* 11, 18 (2021), 8540.
- [28] Jianyang Gao and Cheng Long. 2024. Rabitq: Quantizing high-dimensional vectors with a theoretical error bound for approximate nearest neighbor search. *Proceedings of the ACM on Management of Data* 2, 3 (2024), 1–27.
- [29] Google. [n.d.]. Object storage for companies of all sizes. <https://cloud.google.com/storage>.
- [30] Hao Guo and Youyou Lu. 2025. Achieving {Low-Latency} {Graph-Based} Vector Search via Aligning {Best-First} Search Algorithm with {SSD}. In *19th USENIX Symposium on Operating Systems Design and Implementation (OSDI 25)*. 171–186.
- [31] Rentong Guo, Xiafan Luan, Long Xiang, Xiao Yan, Xiaomeng Yi, Jigao Luo, Qianya Cheng, Weizhi Xu, Jiarui Luo, Frank Liu, et al. 2022. Manu: a cloud native vector database management system. *arXiv preprint arXiv:2206.13843* (2022).
- [32] Gabriel Haas and Viktor Leis. 2023. What modern nvme storage can do, and how to exploit it: High-performance i/o for high-performance storage engines. *Proceedings of the VLDB Endowment* 16, 9 (2023), 2090–2102.
- [33] harsha simhadri. 2024. Big ANN Benchmarks. <https://github.com/harsha-simhadri/big-ann-benchmarks>.
- [34] Binbing Hou, Feng Chen, Zhonghong Ou, Ren Wang, and Michael Mesnier. 2017. Understanding I/O performance behaviors of cloud storage from a client's perspective. *ACM Transactions on Storage (TOS)* 13, 2 (2017), 1–36.
- [35] Piotr Indyk and Hailie Xu. 2023. Worst-case performance of popular approximate nearest neighbor search implementations: Guarantees and limitations. *Advances in Neural Information Processing Systems* 36 (2023), 66239–66256.
- [36] Suhas Jayaram Subramanya, Fnu Devvrit, Harsha Vardhan Simhadri, Ravishankar Krishnamamy, and Rohan Kadekodi. 2019. Diskann: Fast accurate billion-point nearest neighbor search on a single node. *Advances in Neural Information Processing Systems* 32 (2019).
- [37] Hervé Jégou, Romain Tavenard, Matthijs Douze, and Laurent Amsaleg. 2011. Searching in one billion vectors: re-rank with source coding. In *2011 IEEE International Conference on Acoustics, Speech and Signal Processing (ICASSP)*. IEEE, 861–864.
- [38] Yeonwoo Jeong, Hyunji Cho, Kyuri Park, Youngjae Kim, and Sungyong Park. 2025. CALL: Context-Aware Low-Latency Retrieval in Disk-Based Vector Databases. *arXiv preprint arXiv:2509.18670* (2025).
- [39] Yeonwoo Jeong, Kyuri Park, Hyunji Cho, and Sungyong Park. 2025. CaGR-RAG: Context-aware Query Grouping for Disk-based Vector Search in RAG Systems. *arXiv preprint arXiv:2505.01164* (2025).
- [40] Alekh Jindal, Shi Qiao, Hiren Patel, Zhicheng Yin, Jieming Di, Malay Bag, Marc Friedman, Yifung Lin, Konstantinos Karanassos, and Sriram Rao. 2018. Computation reuse in analytics job service at microsoft. In *Proceedings of the 2018 International Conference on Management of Data*. 191–203.
- [41] Yannis Kalantidis and Yannis Avrithis. 2014. Locally optimized product quantization for approximate nearest neighbor search. In *Proceedings of the IEEE conference on computer vision and pattern recognition*. 2321–2328.
- [42] Dingyi Kang, Dongming Jiang, Hanshen Yang, Hang Liu, and Bingzhe Li. 2025. Scalable Disk-Based Approximate Nearest Neighbor Search with Page-Aligned Graph. *arXiv preprint arXiv:2509.25487* (2025).
- [43] Gyusun Lee, Seokha Shin, Wonsuk Song, Tae Jun Ham, Jae W Lee, and Jinkyu Jeong. 2019. Asynchronous {I/O} stack: A low-latency kernel {I/O} stack for {Ultra-Low} latency {SSDs}. In *2019 USENIX Annual Technical Conference (USENIX ATC 19)*. 603–616.
- [44] Conglong Li, Minjia Zhang, David G Andersen, and Yuxiong He. 2020. Improving approximate nearest neighbor search through learned adaptive early termination. In *Proceedings of the 2020 ACM SIGMOD International Conference on Management of Data*. 2539–2554.
- [45] Jie Li, Haifeng Liu, Chuanghua Gui, Jianyu Chen, Zhenyuan Ni, Ning Wang, and Yuan Chen. 2018. The design and implementation of a real time visual search system on JD E-commerce platform. In *Proceedings of the 19th International Middleware Conference Industry*. 9–16.
- [46] Defu Lian, Haoyu Wang, Zheng Liu, Jianxun Lian, Enhong Chen, and Xing Xie. 2020. Lightrec: A memory and search-efficient recommender system. In *Proceedings of the web conference 2020*. 695–705.
- [47] Vasilis Mageirakos, Bowen Wu, and Gustavo Alonso. 2025. Cracking Vector Search Indexes. *arXiv preprint arXiv:2503.01823* (2025).
- [48] Yu A Malkov and Dmitry A Yashunin. 2018. Efficient and robust approximate nearest neighbor search using hierarchical navigable small world graphs. *IEEE transactions on pattern analysis and machine intelligence* 42, 4 (2018), 824–836.
- [49] Srushti Mathur and Aayush Chhabra. 2024. Vector search algorithms: A brief survey. In *2024 4th International Conference on Ubiquitous Computing and Intelligent Information Systems (ICUIIS)*. IEEE, 365–371.
- [50] Nimrod Megiddo and Dharmendra S Modha. 2004. Outperforming LRU with an adaptive replacement cache algorithm. *Computer* 37, 4 (2004), 58–65.
- [51] Meta. [n.d.]. Llama Models. <https://www.llama.com/>.
- [52] Pietro Michiardi, Damiano Carra, and Sara Migliorini. 2019. In-memory Caching for Multi-query Optimization of Data-intensive Scalable Computing Workloads.. In *EDBT/ICDT Workshops*.
- [53] Microsoft. [n.d.]. Azure Blob Storage. <https://azure.microsoft.com/en-us/products/storage/blobs>.
- [54] Microsoft. [n.d.]. Azure subscription and service limits, quotas, and constraints. <https://learn.microsoft.com/en-us/azure/azure-resource-manager/management/azure-subscription-service-limits>.
- [55] Microsoft. [n.d.]. DiskANN - Github. <https://github.com/microsoft/DiskANN>.

[56] Microsoft. [n.d.]. Introducing Phi-3: Redefining what's possible with SLMs. <https://azure.microsoft.com/en-us/blog/introducing-phi-3-redefining-whats-possible-with-slms/>.

[57] Microsoft. [n.d.]. Mount Blob Storage by using the Network File System (NFS) 3.0 protocol. <https://learn.microsoft.com/en-us/azure/storage/blobs/network-file-system-protocol-support-how-to>.

[58] Microsoft. [n.d.]. SPACEV1B: A billion-Scale vector dataset for text descriptors. <https://github.com/microsoft/SPTAG/tree/main/datasets/SPACEV1B>.

[59] Microsoft. [n.d.]. SPTAG - Github. <https://github.com/microsoft/SPTAG>.

[60] Milvus. [n.d.]. IVF-PQ. <https://milvus.io/docs/ivf-pq.md>.

[61] Milvus. [n.d.]. What is the impact of embedding dimension and index type on the performance of the vector store, and how might that influence design choices for a RAG system requiring quick retrievals? <https://milvus.io/ai-quick-reference/what-is-the-impact-of-embedding-dimension-and-index-type-on-the-performance-of-the-vector-store-and-how-might-that-influence-design-choices-for-a-rag-system-requiring-quick-retrievals>.

[62] Jason Mohoney, Anil Pacaci, Shihabur Rahman Chowdhury, Umar Farooq Minhas, Jeffery Pound, Cedric Renggli, Nima Reyhani, Ihab F Ilyas, Theodoros Rekatsinas, and Shivaram Venkataraman. 2024. Incremental IVF Index Maintenance for Streaming Vector Search. *arXiv preprint arXiv:2411.00970* (2024).

[63] Jason Mohoney, Anil Pacaci, Shihabur Rahman Chowdhury, Ali Mousavi, Ihab F Ilyas, Umar Farooq Minhas, Jeffrey Pound, and Theodoros Rekatsinas. 2023. High-throughput vector similarity search in knowledge graphs. *Proceedings of the ACM on Management of Data* 1, 2 (2023), 1–25.

[64] Mark Moshayedi and Patrick Wilkinson. 2008. Enterprise SSDs: Solid-state drives are finally ready for the enterprise. But beware, not all SSDs are created alike. *Queue* 6, 4 (2008), 32–39.

[65] Haechan Noh, Taeho Kim, and Jae-Pil Heo. 2021. Product quantizer aware inverted index for scalable nearest neighbor search. In *Proceedings of the IEEE/CVF International Conference on Computer Vision*. 12210–12218.

[66] nvidia. [n.d.]. TurboPuffer - Architecture. <https://turbopuffer.com/docs/architecture>.

[67] OpenAI. [n.d.]. OpenAI. <https://openai.com/>.

[68] Openmetal. [n.d.]. Big Data for Fraud Detection: A Guide for Financial Services and E-commerce. <https://openmetal.io/resources/blog/big-data-for-fraud-detection-a-guide-for-financial-services-and-e-commerce/>.

[69] Zebin Ren, Krijn Doekemeijer, Padma Apparao, and Animesh Trivedi. [n.d.]. Storage-Based Approximate Nearest Neighbor Search: What are the Performance, Cost, and I/O Characteristics? ([n. d.]).

[70] Guru Pramod Rusum and Sunil Anasuri. 2024. Vector Databases in Modern Applications: Real-Time Search, Recommendations, and Retrieval-Augmented Generation (RAG). *International Journal of AI, BigData, Computational and Management Studies* 5, 4 (2024), 124–136.

[71] Tobias Schmidt, Andreas Kipf, Dominik Horn, Gaurav Saxena, and Tim Kraska. 2024. Predicate caching: Query-driven secondary indexing for cloud data warehouses. In *Companion of the 2024 International Conference on Management of Data*. 347–359.

[72] David Shue, Michael J Freedman, and Anees Shaikh. 2012. Performance isolation and fairness for {Multi-Tenant} cloud storage. In *10th USENIX Symposium on Operating Systems Design and Implementation (OSDI 12)*. 349–362.

[73] Yitong Song, Pengcheng Zhang, Chao Gao, Bin Yao, Kai Wang, Zongyuan Wu, and Lin Qu. 2025. TRIM: Accelerating High-Dimensional Vector Similarity Search with Enhanced Triangle-Inequality-Based Pruning. *arXiv preprint arXiv:2508.17828* (2025).

[74] Yi Su, Dan Feng, Yu Hua, and Zhan Shi. 2019. Understanding the latency distribution of cloud object storage systems. *J. Parallel and Distrib. Comput.* 128 (2019), 71–83.

[75] Pooja Tavallali, Peyman Tavallali, and Mukesh Singhal. 2021. K-means tree: an optimal clustering tree for unsupervised learning. *Journal of Supercomputing* 77, 5 (2021).

[76] TurboPuffer. [n.d.]. TurboPuffer - Agentic AI. <https://turbopuffer.com/docs/namespaces>.

[77] turbopuffer. [n.d.]. turbopuffer - search every byte. <https://turbopuffer.com/>.

[78] UQV. 2024. UQV. <http://staff.itee.uq.edu.au/shenht/UQVIDEO/>.

[79] Jianguo Wang, Xiaomeng Yi, Rentong Guo, Hai Jin, Peng Xu, Shengjun Li, Xiangyu Wang, Xiangzhou Guo, Chengming Li, Xiaohai Xu, et al. 2021. Milvus: A purpose-built vector data management system. In *Proceedings of the 2021 International Conference on Management of Data*. 2614–2627.

[80] Mengzhao Wang, Weizhi Xu, Xiaomeng Yi, Songlin Wu, Zhangyang Peng, Xiangyu Ke, Yunjun Gao, Xiaoliang Xu, Rentong Guo, and Charles Xie. 2024. Starling: An i/o-efficient disk-resident graph index framework for high-dimensional vector similarity search on data segment. *Proceedings of the ACM on Management of Data* 2, 1 (2024), 1–27.

[81] Shucheng Wang, Kaiye Zhou, Zhandong Guo, Qiang Cao, Jun Xu, and Jie Yao. 2024. SIndex: An SSD-based Large-scale Indexing with Deterministic Latency for Cloud Block Storage. In *Proceedings of the 53rd International Conference on Parallel Processing*. 1237–1246.

[82] Xiaohua Wang, Zhenghua Wang, Xuan Gao, Feiran Zhang, Yixin Wu, Zhibo Xu, Tianyuan Shi, Zhengyuan Wang, Shizheng Li, Qi Qian, et al. 2024. Searching for best practices in retrieval-augmented generation. *arXiv preprint arXiv:2407.01219* (2024).

[83] Zeyu Wang, Qitong Wang, Xiaoxing Cheng, Peng Wang, Themis Palpanas, and Wei Wang. 2024. Steiner-hardness: A query hardness measure for graph-based ann indexes. *Proceedings of the VLDB Endowment* 17, 13 (2024), 4668–4678.

[84] Qian Xu, Juan Yang, Feng Zhang, Junda Pan, Kang Chen, Youren Shen, Amelie Chi Zhou, and Xiaoyong Du. 2025. Tribase: A Vector Data Query Engine for Reliable and Lossless Pruning Compression using Triangle Inequalities. *Proceedings of the ACM on Management of Data* 3, 1 (2025), 1–28.

[85] Yuming Xu, Hengyu Liang, Jin Li, Shuotao Xu, Qi Chen, Qianxi Zhang, Cheng Li, Ziyue Yang, Fan Yang, Yuqing Yang, et al. 2023. Spfresh: Incremental in-place update for billion-scale vector search. In *Proceedings of the 29th Symposium on Operating Systems Principles*. 545–561.

[86] Zhengyu Yang, Danlin Jia, Stratis Ioannidis, Ningfang Mi, and Bo Sheng. 2018. Intermediate data caching optimization for multi-stage and parallel big data frameworks. In *2018 IEEE 11th International Conference on Cloud Computing (CLOUD)*. IEEE, 277–284.

[87] Ziyang Yue, Bolong Zheng, Ling Xu, Kanru Xu, Shuhao Zhang, Yajuan Du, Yunjun Gao, Xiaofang Zhou, and Christian S Jensen. 2025. Select Edges Wisely: Monotonic Path Aware Graph Layout Optimization for Disk-Based ANN Search. *Proceedings of the VLDB Endowment* 18, 11 (2025), 4337–4349.

[88] Emanuel Zgraggen, Alex Galakatos, Andrew Crotty, Jean-Daniel Fekete, and Tim Kraska. 2016. How progressive visualizations affect exploratory analysis. *IEEE transactions on visualization and computer graphics* 23, 8 (2016), 1977–1987.

[89] Zili Zhang, Chao Jin, Linpeng Tang, Xuanzhe Liu, and Xin Jin. 2023. Fast, approximate vector queries on very large unstructured datasets. In *20th USENIX Symposium on Networked Systems Design and Implementation (NSDI 23)*. 995–1011.

[90] Xiangyu Zhi, Meng Chen, Xiao Yan, Baotong Lu, Hui Li, Qianxi Zhang, Qi Chen, and James Cheng. 2025. Towards Efficient and Scalable Distributed Vector Search with RDMA. *arXiv preprint arXiv:2507.06653* (2025).

[91] Yijie Zhou, Shengyuan Lin, Shufeng Gong, Song Yu, Shuhao Fan, Yanfeng Zhang, and Ge Yu. 2025. GoVector: An I/O-Efficient Caching Strategy for High-Dimensional Vector Nearest Neighbor Search. *arXiv preprint arXiv:2508.15694* (2025).

[92] Zilliz. [n.d.]. DiskANN: A Disk-based ANNS Solution with High Recall and High QPS on Billion-scale Dataset. <https://zilliz.com/blog/diskann-a-disk-based-anns-solution-with-high-recall-and-high-qps-on-billion-scale-dataset>.

[93] Justin Zobel and Alistair Moffat. 2006. Inverted files for text search engines. *ACM computing surveys (CSUR)* 38, 2 (2006), 6–es.